

Effects of Framing Errors on the Performance of Molecular Communications With Memory

BARIS ATAKAN¹ AND SEBASTIÀ GALMÉS^{2,3}

¹Department of Electrical and Electronics Engineering, Izmir Institute of Technology, 35430 Izmir, Turkey

²Department of Mathematics and Computer Science, University of the Balearic Islands, 07122 Palma, Spain

³Health Research Institute of the Balearic Islands (IdISBa), 07010 Palma, Spain

Corresponding author: Baris Atakan (barisatakan@iyte.edu.tr)

This work was supported by the Scientific and Technological Research Council of Turkey (TUBITAK) under Grant 119E041.


ABSTRACT In conventional digital communication systems, synchronous transmission is achieved by embedding the clocking information into the data signal. However, the implementation of this technique in molecular communication systems, which rely on the diffusion of molecules as information carriers, becomes very complex due to the randomness of the diffusion process. Hence, in this paper we consider the molecular communication between two nanoscale devices with no exchange of any clock signal. To initiate the communication, the transmitter sends a special molecular symbol called beacon in order to trigger the detection process in the receiver. Therefore, this beacon symbol is equivalent to the start bit used for framing in asynchronous serial communication systems. We assume that both transmitter and receiver clocks are perfect, but not synchronized. Accordingly, the analysis focuses on the effects of framing errors on the performance of the molecular channel, measured via the symbol error probability. These errors are inherent to the random nature of the beacon arrival instant, which tends to degrade the alignment between the transmitter and receiver frames. We also assume a molecular channel with any level of inter-symbol interference and the use of different types of molecules to encode information symbols. We validate the derived SEP expression by means of extensive simulation experiments, and finally we develop a design scheme for the beacon symbol that satisfactorily mitigates the effects of framing errors.

INDEX TERMS Molecular communication, symbol framing error, channel memory, beacon message, performance evaluations.

I. INTRODUCTION

Nano and biotechnology currently allow the practical realization of nanomachines (NMs) with tiny components that can accomplish simple sensing and computation tasks. While a single NM has very limited capabilities, the interconnection of NMs in a nanonetwork (NN) can extend their potentials to realize many sophisticated applications. Molecular Communication (MC), in which messenger molecules are used to share information, is a promising alternative for the interconnection of NMs. The concept of MC is introduced in [1], [2]. An extensive survey on nanonetworking with MC is presented in [3]. Furthermore, recent books and survey papers substantially overview the current literature on MC paradigm ([4]–[9]).

A key feature of diffusion-based MC channels, in contrast to traditional radio, optical or electrical communications,

The associate editor coordinating the review of this manuscript and approving it for publication was Di Zhang .

is the fact that propagation delays are random. Emitted molecules randomly diffuse into the medium until eventually reach the receiver at arbitrary instants. This behavior plays a fundamental role in the performance of the molecular channel. Thus, in order to analyze standard performance metrics like noise level, symbol error probability, packet delay or channel capacity, it is very important to accurately describe the dissemination process of a symbol, which is encoded as a group of molecules emitted by the transmitter nanomachine (TN) towards the receiver nanomachine (RN). However, the very limited capabilities of NMs and the random nature of molecular transmission make it almost impossible to realize exact time-synchronization between the TN and the RN. Some recently developed methods try to reproduce this ideal scenario. In general, current mechanisms can be classified into five categories: collective pattern-based techniques, two-way message exchange, one-way message exchange, blind synchronization and partially-untimed schemes.

Collective pattern-based techniques are bio-inspired approaches that imitate the synchronized behavior exhibited by bacteria upon exchanging certain types of molecules. For instance, the work presented in [10] focuses on coordinating the course of action of several NMs by emulating the mechanism of quorum sensing, a biological process by which bacteria are able to adopt a single common behavior that makes them more effective. To achieve this coordination, bacteria secrete a special type of molecules called auto-inducers, which are capable of triggering the release of the same type of molecules by nearby bacteria. Another collective pattern-based mechanism is described in [11], where NMs release inhibitory molecules instead of auto-inducers to create a coordinated oscillation. Inhibitory molecules, once emitted by a NM, restrain the emission of the same kind of molecules by the rest of NMs. Finally, another bio-inspired approach is adopted in [12], where a mechanism based on quorum sensing through two types of auto-inducers is proposed. This mechanism, which has been observed in the *P. Aeruginosa*, induces a collective oscillation between any two specimens of these bacteria (each releasing one type of auto-inducers).

As pointed out by several authors, a big disadvantage of the above bio-inspired approaches is that they try to equalize the length of the oscillation period rather than align the time between the transmitter and receiver clocks. Precisely, the subsequent categories focus on achieving this time alignment. In particular, in the two-way message exchange category, two NMs execute several rounds of control message exchanges until they achieve synchronization. This means that each NM has evaluated some maximum-likelihood estimator (MLE) from the obtained time-stamps. Examples of this two-way approach are [13] and [14]. In the first case, the propagation delay is assumed to follow an inverse Gaussian distribution (channel with drift), whereas in the second case the propagation delay is Gaussian (channel without drift). Another example is [15], which focuses on mobile molecular communication systems. However, in spite of their theoretical support, these proposals exhibit two significant drawbacks as a result of using MLEs. Firstly, due to the low propagation speed that characterizes the molecular channel, the convergence time may be unacceptably large, as typically several tens of rounds are required to achieve accurate estimates. This becomes especially harmful if the synchronization process needs to be refreshed regularly. Secondly, the computational complexity entailed by the calculation of MLEs can largely exceed the capabilities of a single NM.

In order to reduce the overhead of two-way mechanisms, a one-way message exchange is proposed in [16] to estimate the clock offset in a MC channel with drift. In this case, the transmitter records its own clock reading and immediately sends it by using a synchronization message. Upon detecting this message, the receiver records its own clock reading too. The complete process takes several iterations of these single-message transmissions, after which the receiver obtains a set of time-stamp pairs. Again by using some form of MLE, an estimate of the clock offset is obtained. Compared to the

two-way message exchange, the one-way alternative exhibits lower complexity and smaller convergence time, though the resulting synchronization between clocks is less accurate.

A general drawback of the one-way and two-way message exchange mechanisms is that they rely on the knowledge of some relevant channel parameters (diffusion coefficients of messenger molecules and distance between NMs) to implement the MLEs. To avoid this limitation, blind synchronization was proposed in [17]. Blind synchronization does not require any information about the channel, and no time-stamps are exchanged between transmitter and receiver. Rather, the received symbol sequence is directly used to extract clock information. This is achieved by forcing the RN to record the non-regular time instants at which peaks of molecule concentrations corresponding to successive symbols take place. Then, the channel delay (clock offset) is estimated by using a special MLE, called non-decision directed maximum likelihood criterion. Unfortunately, this becomes one of the disadvantages of blind synchronization, as the implementation of such special estimator is very complex. The authors of [18] highlight another drawback of this method, which is the assumption that the clocks of both transmitter and receiver are perfect, have identical frequencies and only a constant clock offset may exist between them. Hence, they propose a blind synchronization mechanism that uses two symbols and suboptimal estimators to determine both clock offset and clock skew from the received sequence, which does not need to be regularly timed (in fact, no clock is assumed at the transmitter side). However, they assume that the receiver periodically samples the incoming signal, which is rather contradictory with their own criticism against the perfectibility of internal clocks. Other disadvantages are the high number of molecules required to encode every symbol in order to mitigate the effects of background noise, and the need to equip the RN with almost as many receptors as molecules for each type of symbol. In [19], another blind scheme is proposed which uses just one symbol for the clock offset estimation without channel knowledge, though combined with single-input multiple-output (MISO) diversity to increase accuracy. However, as the authors of [19] recognize, the proposed method may be too complex for the computing ability of NMs. Finally, another blind scheme is proposed in [20], which proposes a molecular version of the widely used phase locked loop (PLL) to achieve synchronization in conventional electronic systems. However, again the complexity penalizes this scheme.

The last category encompasses mechanisms that are tailored to scenarios where there is no internal clock either at the transmitter or the receiver. These mechanisms are designed to detect the correct sequence of symbols within a reasonable time window, regardless of the specific time instants at which symbols are transmitted. In fact, some of these mechanisms are categorized as asynchronous or synchronization-free. An example is the scheme developed in [21], where the transmitter releases a block of molecular symbols at a constant rate, and then waits for a time period (guard time)

until the next block is sent. In contrast, the receiver is assumed not to be conducted by any internal clock. Accordingly, different detection algorithms are proposed to asynchronously detect molecular information. However, only moderately good values for the bit error rate (BER) are achieved at the expense of very long symbol times, around 600 seconds. The mechanism proposed in [18] also belongs to the partially-untimed category, since the transmitter is neither required to be equipped with an internal clock nor restricted to release the symbols at a regular rate. The results shown in [18] outperform those obtained in [21], because similar values of BER are obtained for much smaller symbol durations (in the order of a few milliseconds). However, these results are achieved under very strong assumptions about inter-symbol interference (ISI). The work presented in [22] proposes a MC scheme with molecular arrays in which the transmission order of two molecule types is considered for binary encoding, thus not requiring any synchronization between transmitter and receiver. Both analysis and simulation yield high transmission rates, though by neglecting background noise and by assuming that ISI takes place only between consecutive symbols. A similar strategy is proposed in [23], where a binary molecule shift keying modulation (MoSK), consisting of mapping bit 0 and bit 1 to a single molecule of type *a* and type *b* respectively, is employed. The receiver performs an asynchronous demodulation that exploits the arrival order of molecules instead of their arrival times.

In [24], an asynchronous communication scheme is developed by randomizing the inter-transmission times of an original type-based synchronous MC system, and utilizing the random inter-transmission times to embed additional information. It is shown that this process, called asynchronous information embedding, significantly increases the capacity of the original system. However, again the receiver design becomes quite complex. Precisely, in [25], a receiver of low structure complexity is proposed, which only has to be equipped with two basic functions, namely molecule discrimination and molecule count. The transmitter uses a pulse position modulation scheme, where information symbols are encoded in the release time of signal molecules. Also, a burst of referential molecules is sent at a predefined time instant within the symbol period, independently of the symbol being transmitted. The receiver does not have any clock and it only has to record the number of signal molecules between every pair of consecutive arrivals of referential molecules. Though in effect the structure complexity of the receiver is reduced, the computational complexity of the decoding process may still be significant, since it relies on maximum likelihood estimators. Moreover, the transmitter is assumed to release both signal and referential molecules at very specific points in the time-slotted axis, thus requiring a very precise oscillator. Finally, two modulation schemes are proposed in [26] which neither require synchronization between transmitter and receiver. This is because information is encoded in the time between two consecutive releases of information particles, either indistinguishable (modulation B in the

paper) or distinguishable (modulation C). It is shown that the asynchronous modulation based on two distinguishable particles exhibits a performance close to the synchronous scheme consisting of encoding information in the time of particle release (system A). However, both transmitter and receiver are assumed to have very precise control on the time interval between two consecutive particles, and again the detection process is based on evaluating MLEs.

In general, the above schemes lead to low symbol transmission rates and have the disadvantage of complexity, even when strong simplifying assumptions are adopted in their conception. Thus, in this paper we consider the molecular communication between two nanoscale devices that have their own internal clocks but do not exchange any clock signal. So, symbols are transmitted according to the transmitter clock and detected according to the receiver clock, in spite of the misalignment between them. Specifically, to initiate the communication, the transmitter sends a special molecular symbol called beacon in order to trigger the detection process in the receiver. Then, if the sequence of symbols is relatively short, this process does not lead to excessive errors in spite of the misalignment between clocks. Definitely, this scheme is the molecular version of the well-known asynchronous serial communication (ASC) used in conventional networks. In particular, the beacon symbol plays the role of the start bit (framing symbol). In addition to the inherent simplicity of this scheme, we believe that it fits into the requirements of many envisaged applications, especially in the field of nanomedicine, as they will probably rely on the exchange of short but effective messages between intra-body NMs.

Our initial evaluation of the proposed molecular ASC (MASC) assumes that both transmitter and receiver clocks are perfect, though not synchronized. In this way, we can focus exclusively on how beacon detection errors affect the correct detection of subsequent information symbols (via the symbol error probability - SEP). These framing errors are inherent to the random nature of the beacon arrival instant, which generally causes an undesirable shift between the actual and the ideal detection instants of information symbols. For the sake of generality, we consider a multilevel molecular encoding scheme, where each symbol is represented by a type of chemical compound. We note however that it is the complexity of implementation that will finally dictate plausible values for the number of symbols. We also assume a realistic molecular channel with any level of ISI. Then, on the basis of these assumptions, we obtain a performance function that maps beacon synchronization errors (framing errors) into information symbol errors (via the SEP). Finally, we set up the guidelines to properly design the beacon symbol such that SEP is kept very small. This design entails the selection of the emission level and diffusion coefficient of the beacon molecules. At this point, we note that the parameter selection performed in this paper is based only on communication criteria, but other factors should also be considered when transiting from theory to practice. For instance, the work presented in [27] highlights the extremely high

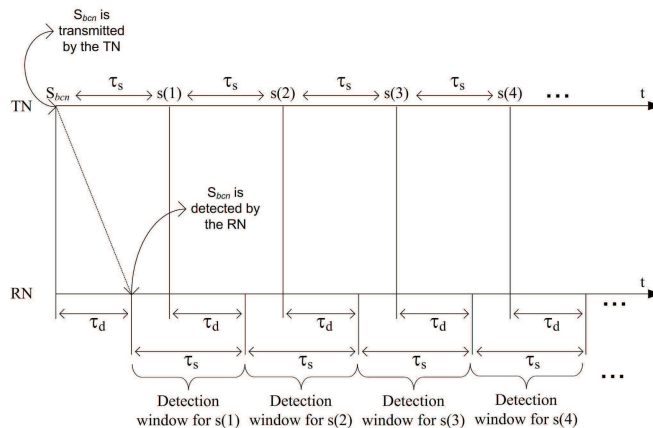


FIGURE 1. Timing diagram for the molecular channel under a framing error.

human safety requirements imposed on the operation of in-body nanonetworks for biomedical applications, whereas the risk of altering the equilibrium between the biosphere and the atmosphere, as a consequence of human-driven changes in the emission levels of the so-called biogenic volatile organic compounds (BVOC), is discussed in [28].

The remainder of the paper is organized as follows. In Section II, the delay distributions of the beacon and information symbols are first derived. Then, based on these distributions, the symbol error probability (SEP) is obtained as a function of the beacon detection instant. In Section III, a design scheme for the beacon symbol is introduced in order to obtain very small values for SEP. The derived SEP expression is validated by means of extensive simulation experiments in Section IV. Numerical results, including comparisons between the proposed MASC and an ideal scheme with perfect synchronization, are presented in Section V. Finally, in Section VI, concluding remarks and suggestions for further research are outlined.

II. MOLECULAR COMMUNICATION UNDER A FRAMING ERROR

An M -ary MC scheme is considered, in which each symbol S_a is transmitted by emitting N_a molecules of type ψ_a , where $a \in \{1, \dots, M\}$. With no detriment on the main objective of this paper, which is the viability of a fully asynchronous molecular communication scheme, the medium is assumed to be one-dimensional for simplicity. In fact, the obtained results can be easily extended to the 3D case by simply modifying the mathematical expressions of the input distributions (hitting time distributions), fact that does not cause any change in the analytical formulation of SEP. On the other hand, the 1D case is consistent with many scenarios, such as a nanonetwork deployed in a water pipe, an oil pipeline or the human cardiovascular system. Regarding the emission of molecules, it is performed by the Transmitter Nanomachine (TN) in each inter-symbol time τ_s , as illustrated by the timing diagram in Fig. 1, where $s(i)$ denotes the i^{th} symbol, that is,

$s(i) = S_a, a \in \{1, \dots, M\}, i \in \{1, \dots\}$. The Receiver Nanomachine (RN) is assumed to detect the symbols by distinguishing and counting the received molecules. This detection is accomplished through a pre-specified threshold σ_a , meaning that the symbol S_a is correctly received if at least σ_a molecules of type ψ_a are detected within the inter-symbol time τ_s , and the rest of symbols do not exceed their thresholds.

Any transmitted symbol is assumed to be affected by m previous symbols, where m is the level of channel memory.¹ For example, if $m = 20$, this means that any symbol transmission is affected by the previous twenty symbols. The communication between the TN and RN is triggered by a specific symbol called beacon, which is denoted by S_{bcn} as illustrated in Fig. 1. The beacon symbol is encoded by a certain type of molecule ψ_{bcn} , different from those used for the encoding of information symbols. This molecule type is characterized by a diffusion coefficient, namely D_{bcn} . The emission level associated to this symbol is N_{bcn} and the corresponding detection threshold is σ_{bcn} . After the TN transmits the beacon symbol at $t = 0$, the RN detects it at the random time $t = \tau_d$ when it collects σ_{bcn} molecules. Then, the MC between the TN and RN is initiated at time $t = \tau_d$ without fixing the timing offset, which causes a framing error. This is shown in Fig. 1. The cumulative distribution function of the random delay of the beacon message, i.e., τ_d , can be given as

$$F_{\tau_d}(t) = Pr(\tau_d \leq t) = \sum_{i=\sigma_{bcn}}^{N_{bcn}} \binom{N_{bcn}}{i} [F_{bcn}(t)]^i \times [1 - F_{bcn}(t)]^{N_{bcn}-i}, \quad (1)$$

where $F_{bcn}(t)$ denotes the distribution function of the delay experienced by any molecule encoding the beacon. This is given by the following expression [29]:

$$F_{bcn}(t) = \text{erfc}\left(\frac{d}{\sqrt{4D_{bcn}t}}\right), \quad t > 0, \quad (2)$$

¹Since such a channel memory causes ISI, the terms ‘‘ISI memory’’ or ‘‘ISI window’’ can be used interchangeably.

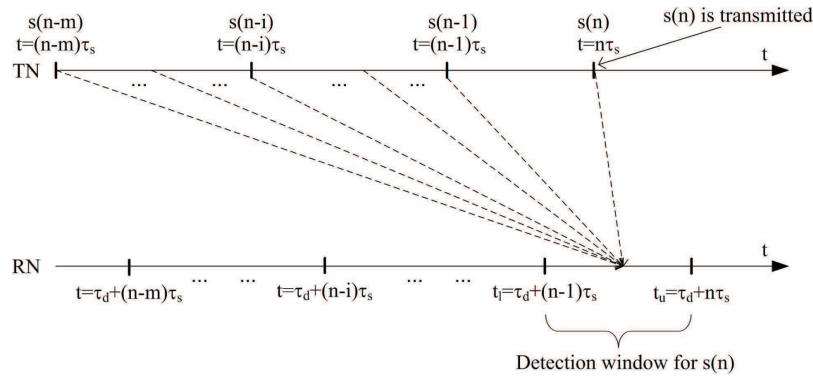


FIGURE 2. Timing diagram for the transmission and detection of symbol $s(n)$.

where $\text{erfc}(\cdot)$ and d denote the complementary error function and the distance between the TN and the RN, respectively. The probability density function and the mean of τ_d can be written as follows:

$$f_{\tau_d}(t) = \frac{d}{dt} F_{\tau_d}(t), \tag{3}$$

$$E[\tau_d] = \int_0^\infty t f_{\tau_d}(t) dt. \tag{4}$$

After the beacon symbol is detected at $t = \tau_d$, the RN starts to count molecules during each inter-symbol time τ_s and decides if the threshold $\sigma_a, a \in \{1, \dots, M\}$ is exceeded by a particular type at the end of τ_s (see Fig. 1) (while the rest of thresholds are not being exceeded). Let us define the counting process $r_a(N_a, t)$, which stands for the number of molecules of type ψ_a that have hit the RN until time t , given that N_a molecules were emitted at $t = 0$. The probability mass function associated with this process, $\phi_a(N_a, l, t)$, is the probability that exactly l molecules have reached the RN at time t , given that a set of N_a molecules were emitted at $t = 0$. It is as follows:

$$\begin{aligned} \phi_a(N_a, l, t) &= \Pr(r_a(N_a, t) = l) \\ &= \binom{N_a}{l} [F_{\psi_a}(t)]^l \\ &\quad \times [1 - F_{\psi_a}(t)]^{N_a-l}. \end{aligned} \tag{5}$$

Here, $l \in [0, N_a], t \geq 0$ and $F_{\psi_a}(t)$ is the cumulative distribution function of the delay experienced by any single molecule ψ_a to reach the RN. It is given by [29]

$$F_{\psi_a}(t) = \text{erfc}\left(\frac{d}{\sqrt{4D_{\psi_a}t}}\right), \quad t > 0, \tag{6}$$

where D_{ψ_a} is the diffusion coefficient of molecule type ψ_a .

Let us now focus on the n^{th} symbol $s(n) = S_a, a \in \{1, \dots, M\}$. Symbol $s(n)$ is transmitted at time $t = n\tau_s$ by the TN by emitting N_a molecules of type ψ_a . Due to the timing offset τ_d , the RN tries to detect $s(n)$ within the interval from $t_l = \tau_d + (n-1)\tau_s$ to $t_u = \tau_d + n\tau_s$ as illustrated in Fig. 2. Here, t_l and t_u denote the lower and upper limits of

the detection interval of symbol $s(n)$, respectively. Note that t_u can be expressed as $t_u = t_l + \tau_s$.

Depending on the magnitude of the timing offset τ_d , the symbols interfering within the detection interval of symbol $s(n)$ vary. These interfering symbols may be predecessor symbols like $s(n-1), s(n-2) \dots$ and/or successor symbols like $s(n+1), s(n+2) \dots$. More specifically, depending on the magnitude of τ_d , the interfering symbols can be identified as follows:

- If $0 < \tau_d \leq \tau_s$, the molecules belonging to symbols $s(n), s(n-1), \dots, s(n-m)$ may reach the RN within the interval $[t_l, t_u]$. Recall that m is the memory level of the channel.
- If $\tau_s < \tau_d \leq 2\tau_s$, the molecules of symbols $s(n+1), s(n), s(n-1), \dots, s(n-m+1)$ may reach the RN.
- If $2\tau_s < \tau_d \leq 3\tau_s$, the molecules of symbols $s(n+2), s(n+1), s(n), \dots, s(n-m+2)$ may reach the RN.
- ⋮
- If $m\tau_s < \tau_d \leq (m+1)\tau_s$, the molecules of symbols $s(n+m), s(n+m-1), s(n+m-2), \dots, s(n)$ may reach the RN. This is the last chance for the molecules of symbol $s(n)$ to reach the RN; if τ_d further increases while m remains fixed, it is no longer possible that such molecules reach the RN.

In general, if $k\tau_s < \tau_d \leq (k+1)\tau_s$, then the symbols interfering with $s(n)$ can be expressed as $s(n+k-i), k \in \{0, \dots, m\}, i \in \{0, \dots, m\}$. Note that for the case $i = k$, symbol $s(n+k-i)$ becomes $s(n)$.

The next step is to characterize how many molecules belonging to symbol $s(n+k-i)$ can reach the RN within $[t_l, t_u]$. Let us assume that $s(n) = S_a$. If symbol $s(n+k-i)$, with $i \neq k$, is equal to symbol S_a , then it can help symbol $s(n) = S_a$ to exceed its threshold σ_a . Otherwise, it does not affect the detection of symbol $s(n) = S_a$. Hence, the random variable $e_{k,i}^a$ denoting the amount of molecules of type ψ_a coming from symbol $s(n+k-i)$, with $i \neq k$, can be formulated as

$$e_{k,i}^a = \begin{cases} c_{k,i}^a, & s(n+k-i) = S_a, \quad i \neq k \\ 0, & s(n+k-i) = S_b, \quad b \neq a, \quad i \neq k, \end{cases} \tag{7}$$

where $c_{k,i}^a$ is a random variable that stands for the number of molecules ψ_a that were emitted at time $t = (n + k - i)\tau_s$, with $i \neq k$, and reach the RN during the detection interval of symbol $s(n)$. Note that the condition $i \neq k$ means that $e_{k,i}^a$ excludes the contribution of current symbol $s(n)$. The probability mass function corresponding to $c_{k,i}^a$ is the probability that exactly l molecules reach the RN within $(t_l, t_u]$, given that N_a molecules were emitted at time $t = (n + k - i)\tau_s$, with $i \neq k$. It is given by

$$\varphi_{k,i}^a(l, \tau_d) = \binom{N_a}{l} [p_{k,i}^a(\tau_d)]^l [1 - p_{k,i}^a(\tau_d)]^{N_a-l}, \quad (8)$$

where $p_{k,i}^a(\tau_d)$ is the probability that a molecule of type ψ_a emitted at time $t = (n + k - i)\tau_s$ reaches the RN during $(t_l, t_u]$. It can be expressed as:

$$p_{k,i}^a(\tau_d) = F_{\psi_a}[t_u - (n+k-i)\tau_s] - F_{\psi_a}[t_l - (n+k-i)\tau_s]. \quad (9)$$

Note that since t_u and t_l are respectively given by $t_u = \tau_d + (n - 1)\tau_s$ and $t_l = \tau_d + (n - 2)\tau_s$, equation (9) can also be written as

$$p_{k,i}^a(\tau_d) = F_{\psi_a}[\tau_d - (k-i)\tau_s] - F_{\psi_a}[\tau_d - (k-i+1)\tau_s]. \quad (10)$$

Now, by using the probability mass function of $c_{k,i}^a$ in (8), we can develop the probability mass function of $e_{k,i}^a$, i.e. $\tilde{\varphi}_{k,i}^a(l)$, as follows:

$$\tilde{\varphi}_{k,i}^a(l, \tau_d) = \frac{1}{M} \varphi_{k,i}^a(l, \tau_d) + \frac{M-1}{M} \delta(l), \quad (11)$$

where $l = 0, \dots, N_a$ and $\delta(\cdot)$ is the delta function. In addition to the molecules included in the counting variable $e_{k,i}^a$, the RN also receives the molecules emitted by the current symbol, i.e. $s(n) = S_a$. So, let g_k^a denote the number of molecules ψ_a that reach the RN within $(t_l, t_u]$, given that symbol $s(n) = S_a$ is emitted at time $t = n\tau_s$. Then, the probability mass function of g_k^a can be given by

$$\vartheta_k^a(l, \tau_d) = \binom{N_a}{l} [q_k^a(\tau_d)]^l [1 - q_k^a(\tau_d)]^{N_a-l}, \quad (12)$$

where $q_k^a(\tau_d)$ is the probability that a molecule of type ψ_a , which is emitted at time $t = n\tau_s$ as part of symbol $s(n) = S_a$, reaches the RN within $(t_l, t_u]$. Similar to (9), it can be expressed as

$$\begin{aligned} q_k^a(\tau_d) &= F_{\psi_a}[t_u - n\tau_s] \\ &\quad - F_{\psi_a}[t_l - n\tau_s] \\ &= F_{\psi_a}[\tau_d] - F_{\psi_a}[\tau_d - \tau_s]. \end{aligned} \quad (13)$$

Now, for a given k , which means $k\tau_s < \tau_d \leq (k+1)\tau_s$, $k \in \{0, \dots, m\}$, the total number of molecules of type ψ_a that reach the RN, i.e. h_k^a , can be written as

$$h_k^a = g_k^a + \sum_{\substack{i=0 \\ i \neq k}}^m e_{k,i}^a. \quad (14)$$

By employing the probability mass functions of $e_{k,i}^a$ and g_k^a , given respectively in (11) and (12), the probability mass function of h_k^a , i.e. $\varrho_k^a(l)$, can be formulated as

$$\varrho_k^a(l, \tau_d) = \vartheta_k^a(l, \tau_d) * \tilde{\varphi}_k^a(l, \tau_d), \quad (15)$$

where $*$ denotes the convolution operation and $\tilde{\varphi}_k^a(l, \tau_d)$ obeys the following expression:

$$\tilde{\varphi}_k^a(l, \tau_d) = \tilde{\varphi}_{k,0}^a(l, \tau_d) * \dots * \tilde{\varphi}_{k,i \neq k}^a(l, \tau_d) * \dots * \tilde{\varphi}_{k,m}^a(l, \tau_d). \quad (16)$$

All convolutions are with respect to the first variable (l). Note that it has been emphasized the fact that $i \neq k$ in the above convolution. Now, let us define the following two probabilities:

$$P_k^a(\tau_d) = \sum_{l=\sigma_a}^{(m+1)N_a} \varrho_k^a(l, \tau_d), \quad (17)$$

$$Q_k^b(\tau_d) = \sum_{l=\sigma_b}^{mN_b} \tilde{\varphi}_k^b(l, \tau_d). \quad (18)$$

Equation (17) corresponds to the probability that symbol S_a exceeds its threshold given that this is the symbol transmitted in the current slot (slot n). On the other hand, expression (18) is the probability that symbol S_b , with $b \neq a$, exceeds its threshold despite it has not been transmitted during the current slot. Accordingly, the probability that symbol S_a is not correctly received can be expressed as follows:

$$SEP(a, \tau_d) = 1 - P_k^a(\tau_d) \prod_{\substack{b=1 \\ b \neq a}}^M [1 - Q_k^b(\tau_d)]. \quad (19)$$

This symbol error probability corresponds to a given τ_d (and hence a given k). By un-conditioning with respect to τ_d , the final expression for the symbol error probability of symbol S_a is given by the following integral, where $f_{\tau_d}(t)$ obeys expression (3):

$$SEP(a) = \int_0^\infty SEP(a, \tau_d) f_{\tau_d}(t) dt. \quad (20)$$

In our implementation, this integral is evaluated (in *Mathematica*) by dividing the area under the curve in many small rectangles. Two control parameters are used:

- Parameter κ , which represents the width of rectangles, that is, the granularity level.
- Parameter γ , which represents the number of rectangles, that is, the number of sampling points.

The smaller the first parameter and the larger the second one, the more accurate the integral evaluation is. To decide the values of these parameters, we also evaluate the integral of expression (3) by using the same mechanism based on rectangles. This integral should converge to 1, since it represents the area of a probability density function. Therefore, the criteria to select κ and γ is that such integral is as close as possible to 1. This must be traded off with the computation

time of the symbol error probability given by expression (20), which depends on the number of points considered in the evaluation (γ). Next, a design scheme is introduced to select the parameters of the beacon message, namely emission level N_{bcn} and diffusion coefficient D_{bcn} .

III. DESIGN OF THE BEACON MESSAGE

Equation (20) is the integral of a function consisting of multiplying $SEP(a, \tau_d)$ by $f_{\tau_d}(t)$. The smaller this product is, the smaller the resulting value for $SEP(a)$ is too. Here, it is very crucial to realize that, whereas $SEP(a, \tau_d)$ depends on the information symbols, $f_{\tau_d}(t)$ only depends on the beacon symbol; accordingly, the two functions can be managed separately in order to make its product as small as possible. Next, we check the behavior of such two functions. For instance, Fig. 3, depicts the evolution of $SEP(a, \tau_d)$ as a function of τ_d (in sec.), for $M = 4$, $D_a = \{1000, 1100, 1200, 1300\} \mu m^2/s$, $N_a = \{40, 39, 38, 37\}$, $\sigma_a = \{14, 14, 14, 14\}$, $m = 5$, $d = 0.6 \mu m$, $\tau_s = 7ms$ and $a = 1$. These values have been taken from our previous contribution [30], which focused on the characterization of the performance effects of any level of ISI window and the parameter selection that optimizes these effects. As it can be noticed, there is a flat region where the symbol error probability is very small. This region is defined between some relatively small value of the beacon delay and a beacon delay equal to, precisely, $7ms$ (the value of τ_s). At this point, a sharp increase towards another flat, but undesired region, takes place. In fact, we have observed this behavior for multiple parameter settings and all information symbols: the evolution of SEP exhibits a window of advantageous values for the symbol delay between a very small value and an upper limit given by τ_s . Here, it is important to note that the performance of the MC with the framing error will be the same as the MC under perfect synchronization when $\tau_d = \tau_s$. This can be easily validated in the diagram shown in Fig. 1.

In order to obtain a small value for the symbol error probability of symbol S_1 , the probability density function of the beacon delay should mostly fall within the desired flat window shown in Fig. 3. This requirement can be extrapolated to the rest of symbols. Hence, a sufficiently narrow probability density function, approximately centered in the midpoint of all desired windows, is recommended. For instance, the probability density function of τ_d is shown in Fig. 4 for four different selections of the diffusion coefficient of the beacon message diffusion. As observed, for $D_{bcn} = 20, 30, 40 \mu m^2/s$, very small SEP values are obtained since the corresponding probability density functions fall almost entirely into the desired flat region of Fig. 3. However, for $D_{bcn} = 10 \mu m^2/s$, the probability density function of τ_d hardly overlaps with the reference window and the resulting SEP is very high (55.23% as shown in the figure).

Fortunately, with the use of a beacon symbol different from those targeted to convey information, the probability density function of the delay until the receiving process starts can be conveniently located within the window shown in Fig. 3

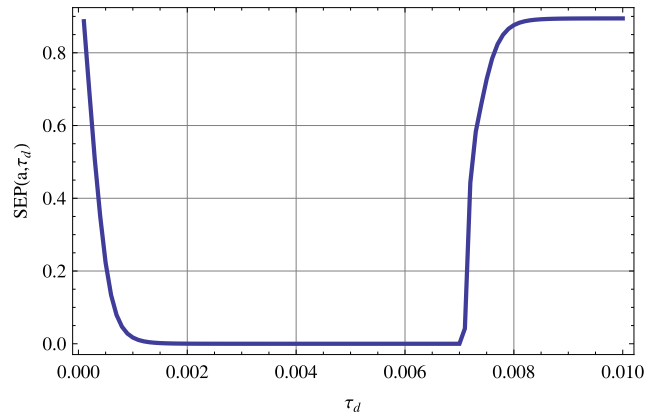


FIGURE 3. Evolution of SEP for the first symbol in terms of the beacon delay.

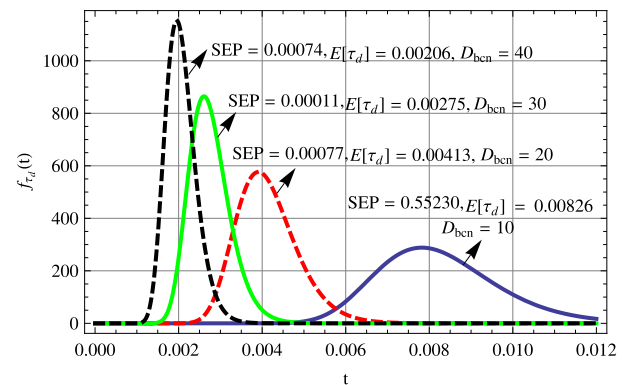


FIGURE 4. Four examples of probability density function of the beacon delay. The diffusion coefficients of the beacon message for such examples are set as $D_{bcn} = 10, 20, 30, 40 \mu m^2/s$.

(for symbol S_1 , but equally for the rest of symbols). At this point, we can summarize some relevant results derived from an exhaustive set of experimental tests:

- Regarding the evolution of $SEP(a, \tau_d)$ in (19), which only depends on the parameters of the information symbols, it always shows a desired flat region between a very small value and an upper limit. The former slightly increases as the value of τ_s increases and, more specially, as the value of distance (d) increases. With respect to the upper limit, it always corresponds to the value of τ_s .
- Regarding the distribution of the beacon delay for a given transmission distance, its expectation can be controlled through the diffusion coefficient and emission level of the molecules that encode the beacon symbol, whereas its squared coefficient of variation (directly related with the amplitude of such distribution) can be controlled by means of the emission level exclusively. So, in order to fix the location and amplitude of the probability density function of the beacon symbol, it is first recommended to adjust the emission level in order to achieve the desired amplitude, and then use the diffusion coefficient to set the final location.

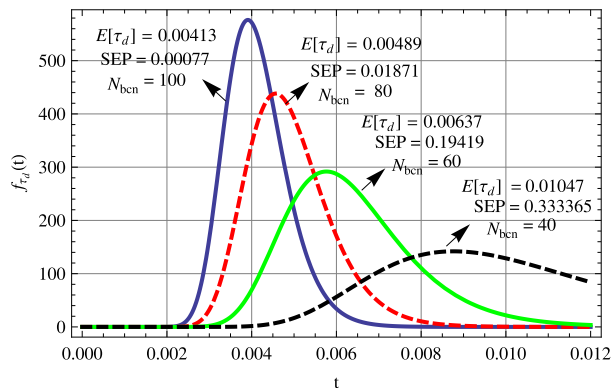


FIGURE 5. Four examples of probability density function of the beacon delay. The emission levels of the beacon message for such examples are set as $N_{bcn} = 100, 80, 60, 40$.

In Figs. 4 and 5, the expected value of the beacon delay ($E[\tau_d]$ in (4)) is shown for different selections of the diffusion coefficient D_{bcn} and the emission level N_{bcn} , respectively. As explained above, by using appropriate values for these parameters, the probability density function of τ_d can be almost completely inscribed into the desired flat region. Particularly, with regard to setting the appropriate value for the diffusion coefficient of the beacon symbol, we expect that the high variety of molecule types (natural or synthetic), combined with the flexibility allowed by the wideness of the flat region, will make it feasible to achieve an optimal or at least suboptimal selection for the beacon molecules. Hence, it is possible to obtain a very small average SEP for any parameter setting regarding information symbols (cardinality, diffusion coefficients, emission levels and thresholds), transmission distance, inter-symbol time and ISI window (channel memory). In the next section, we validate the analytical results via simulation.

IV. VALIDATION OF THE PERFORMANCE ANALYSIS

In this section, the symbol error probability in (20) is validated through extensive simulation experiments. In the validations, the delays experienced by the participating molecules are reproduced by sampling the corresponding distributions of these delays. Then, by applying a procedure essentially based on count data and comparisons with detection thresholds, the SEP variables are numerically computed and compared with the corresponding analytically-obtained SEP values. Four different parameter settings are used for the validation. They are denoted as $ST_i, i \in \{1, 2, 3, 4\}$ and given in Table 1. In these settings, the diffusion coefficients, emission levels and detection thresholds of the 6 symbols used at most are respectively given by $\{1000, 1100, 1200, 1300, 1400, 1500\} \mu m^2/s$, $\{40, 39, 38, 37, 36, 35\}$ and $\{14, 14, 14, 14, 14, 14\}$ (when $M = 4$, only the four initial values in every set are used). For the beacon message, we update D_{bcn} and N_{bcn} as the slot time (τ_s) changes from 0.1 to 0.5 ms (in steps of 0.1). This update is performed according to the bea-

TABLE 1. Parameter settings for the validation of SEP in (20).

Sets	M	m	d
ST_1	4	5	0.75
ST_2	4	5	1
ST_3	4	11	0.75
ST_4	6	5	0.75

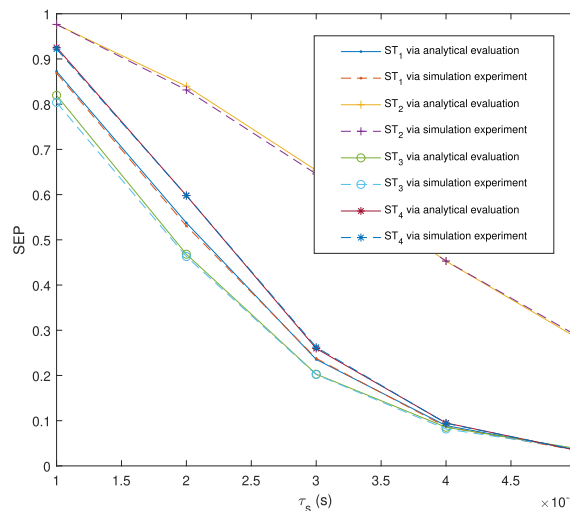


FIGURE 6. Validation of the SEP expression given in (20) via simulation, for the four parameter settings introduced in Table 1.

con message design procedure discussed in the preceding section. For the parameter sets ST_1 and ST_3 , the updated values of D_{bcn} and N_{bcn} are $D_{bcn} = 220, 188, 153, 85, 52$ and $N_{bcn} = 650, 650, 650, 3000, 10000$, respectively; for ST_2 , $D_{bcn} = 220, 217, 200, 177, 157$ and $N_{bcn} = 650$ for all values of τ_s ; finally, for the setting ST_4 , $D_{bcn} = 220, 200, 163, 85, 54$ and $N_{bcn} = 650, 650, 650, 3000, 10000$.

For each parameter setting ($ST_i, i \in \{1, 2, 3, 4\}$) and each slot time (τ_s), SEP is obtained in an analytical way by evaluating equation (20) and via simulation by applying the procedure just described in this section. The comparison between analytical and simulation results is illustrated in Fig. 6. As observed in the figure, analytical and simulation results are very close to each other. This reveals that the analytical derivations are valid.

V. PERFORMANCE EVALUATION

In this section, we evaluate the performance of a molecular channel subject to framing errors and arbitrary lengths of the ISI window (level of memory). Furthermore, we compare this performance with that of a molecular channel under the same conditions regarding the ISI window, but without framing errors (the TN and RN are assumed to be synchronized with each other). The consideration of an arbitrary ISI window (as opposed to the methods described in the review of literature) converts the latter into the synchronous counterpart of

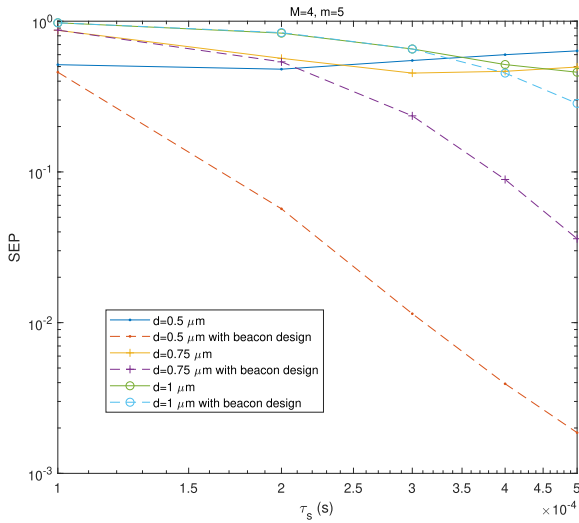


FIGURE 7. SEP of the molecular channel with a framing error for two cases: in the first case, the SEP values are obtained by using just a pair of constant D_{bcn} and N_{bcn} for all distance values and inter-symbol times; in the second case, appropriate values for D_{bcn} and N_{bcn} are selected for each combination of distance and inter-symbol time.

the proposed mechanism, and thus an optimal reference for comparison.

In Fig. 7, it is shown how SEP can be reduced by appropriately regulating the diffusion coefficient of the beacon message (D_{bcn}). The test is done for different values of the distance (d) and by setting $M = 4, m = 5$ and the rest of data as in the previous section (diffusion coefficients, emission levels and thresholds). For the beacon symbol, two cases are considered:

- In the first case, the diffusion coefficient, emission level and detection threshold of the beacon symbol remain constant for all tests, that is, for all combinations of distance and inter-symbol time. Their values are arbitrarily selected with the only criterion of being close to the values used for the information symbols: $D_{bcn} = 1000$, $N_{bcn} = 50$ and $\sigma_{bcn} = 14$.
- In the second case, the values of D_{bcn} and N_{bcn} are appropriately selected as d and τ_s change by following the method introduced in Section III.

As observed in the figure, the beacon message design scheme can significantly reduce the SEP values with respect to those obtained without any adjustment. In order to understand the reason of this phenomenon, let us recall that the MC scheme with a framing error has the same performance as the synchronous communication when the delay of the beacon symbol (τ_d) and the inter-symbol time (τ_s) are the same. Therefore, the performance of the former can be improved as the expectation of τ_d ($E[\tau_d]$) becomes closer to τ_s . In Fig. 7, for the case of constant D_{bcn} and N_{bcn} (no adjustment), which results in a constant $E[\tau_d]$, the inconsistency between the $E[\tau_d]$ and τ_s increases as τ_s grows. Then, this escalates to the SEP values. However, for the case in which D_{bcn} and N_{bcn} are appropriately selected according to the proposed design

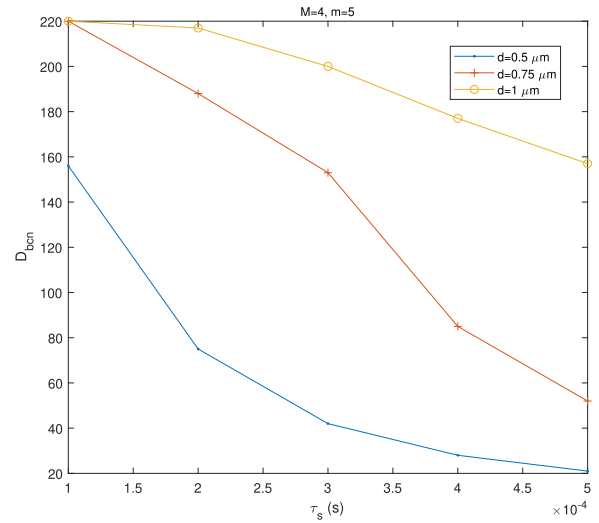


FIGURE 8. Evolution of D_{bcn} as d and τ_s change in Fig. 7.

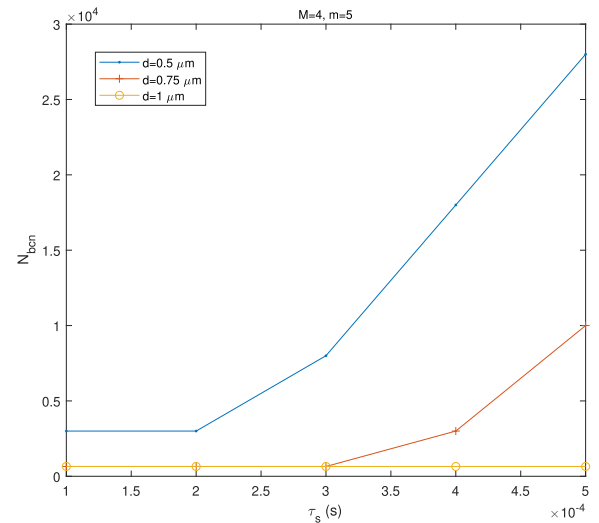


FIGURE 9. Evolution of N_{bcn} as d and τ_s change in Fig. 7.

scheme, the inconsistency between $E[\tau_d]$ and τ_s can be controlled and, correspondingly, the SEP values can be kept very close to those obtained under synchronous communication for all values of τ_s .

The selected values for D_{bcn} and N_{bcn} in Fig. 7 are shown in Figs. 8 and 9, respectively. The values of D_{bcn} increase with d . In effect, as d increases, the beacon molecules need to diffuse more quickly into the medium in order to guarantee the consistency between $E[\tau_d]$ and τ_s . On the other hand, D_{bcn} needs to be decreased as τ_s increases, because slowing down the beacon molecules contributes to maintain the consistency between $E[\tau_d]$ and τ_s . Regarding the evolution of N_{bcn} , let us first take into account the following observations: the variance of τ_d increases as N_{bcn} decreases (as stated in Section III), and the variance of τ_d increases as τ_s increases, because larger inter-symbol times allow for larger variations of the arrival times of beacon molecules at the RN.

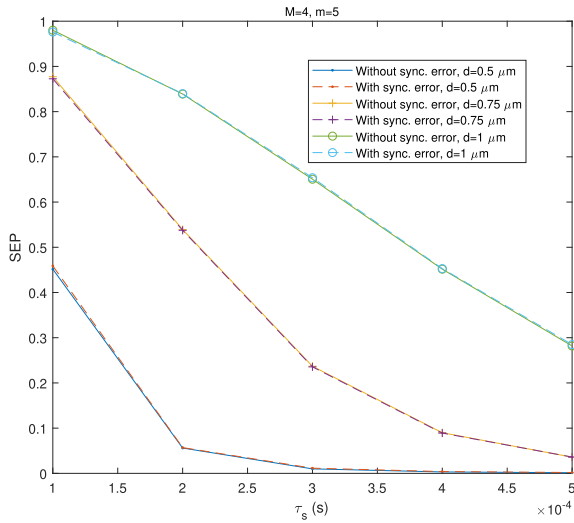


FIGURE 10. Comparison between the MC schemes with and without framing errors for different values of d as τ_s changes.

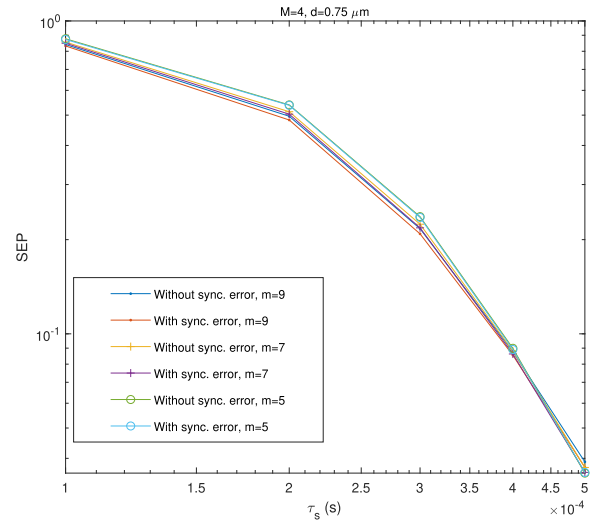


FIGURE 12. Comparison between the MC schemes with and without framing errors for different values of m as τ_s changes (logarithmic scales).

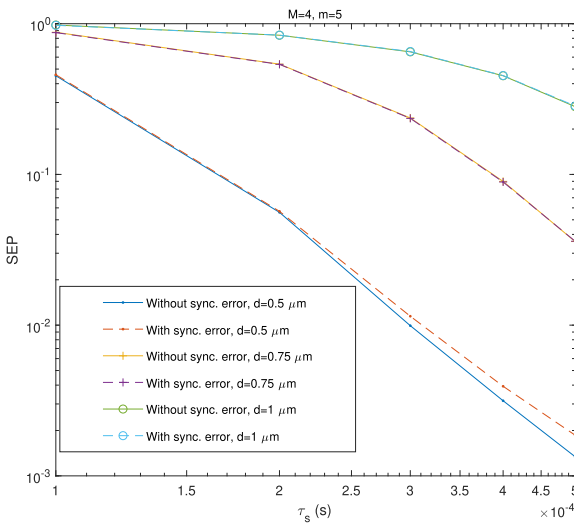


FIGURE 11. Comparison between the MC schemes with and without framing errors for different values of d as τ_s changes (logarithmic scales).

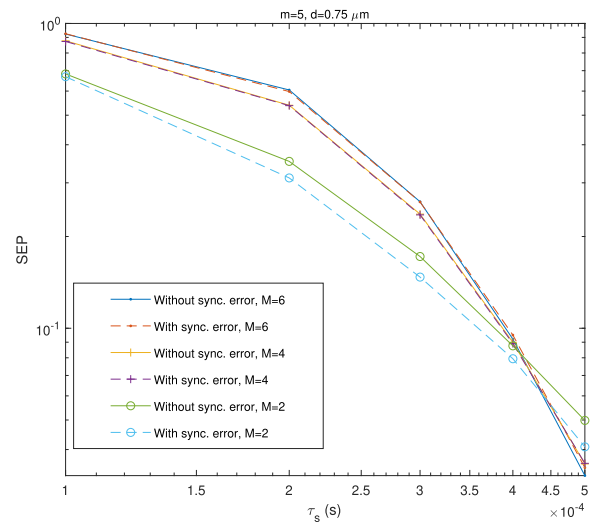


FIGURE 13. Comparison between the MC schemes with and without framing errors for different values of M as τ_s changes (logarithmic scales).

Accordingly, N_{bcn} needs to be increased with τ_s in order to maintain the distribution of τ_d within the flat region of each symbol (recall Fig. 3 for symbol S_1).

In Fig. 10, the MC schemes with and without framing errors are compared in terms of SEP by applying the same setting used in Fig. 7. Schemes with framing errors are assumed to benefit from the beacon design scheme proposed in this paper; schemes without framing errors correspond to perfectly synchronized transmissions. As it can be noticed, the beacon design allows for significantly mitigating the negative effects of framing errors, as the SEP values resulting from both types of transmissions, with and without framing errors, are very close to each other. However, if logarithmic instead of linear scales are used, as shown in Fig. 11, we can observe a slight degradation of the molecular channel with framing errors as τ_s increases. This is due to the difficulty

in adjusting the beacon symbol for large inter-symbol times; actually, we could further reduce such degradation by using very large N_{bcn} and very small D_{bcn} values, but this might not be practical. For example, for the scenario of Fig. 11 in which $d = 0.5 \mu m$ and $\tau_s = 0.0005 s$, N_{bcn} and D_{bcn} are set to 28000 and 21, respectively; in order to match even lower SEP values, N_{bcn} and D_{bcn} should be further increased and decreased, respectively, which may not be feasible from a practical point of view. Anyway, since the slight degradation takes place for the large values of the inter-symbol time, which correspond to the lower transmission rates, its impact is less important.

Similar comparisons between the MC schemes with and without framing errors are presented in Figs. 12 and 13 by slightly modifying the parameter setting of Fig. 11. Specifically, in Fig. 12, $M = 4$ and $d = 0.75 \mu m$, and different values

of the ISI window (m) are considered; in Fig. 13, $m = 5$ and $d = 0.75\mu\text{m}$, and different values of the number of symbols (M) are applied. In all cases, by selecting appropriate values for the parameters of the beacon symbol, the performance of the MC scheme with framing errors closely approaches that of a perfectly synchronized channel. These results reveal that clock synchronization may not be required in molecular communication if a beacon symbol is introduced and properly designed.

VI. CONCLUSION

In this paper, the molecular version of the well-known ASC (asynchronous serial communication) mechanism, namely MASC, has been proposed and investigated. Whereas in ASC the relative clock drift (clock skew) between transmitter and receiver is the only component of de-synchronization, in MASC, due to the randomness of the propagation delay, both clock skew and clock offset need to be considered. Moreover, they must be treated in statistical sense. This paper has focused exclusively on clock offset, which is related to the detection instant of the beacon symbol (the molecular version of the start bit). Specifically, the effects of deviations of the actual with respect to the ideal beacon detection instant have been analyzed. This analysis has been carried out under realistic conditions by considering a molecular channel with an arbitrary ISI window (level of memory). Different types of molecules have been used to encode and send the information symbols as well as the beacon symbol. The delay distributions of the beacon and information symbols have been first derived. Then, based on these distributions, the symbol error probability has been obtained as a function of the beacon detection instant. This result has been validated via extensive simulations. The performance results have shown that SEP is highly affected by how the beacon symbol is designed. Thus, a design scheme for the beacon symbol has been introduced in order to obtain very small values for SEP. In fact, it has been shown that a proper selection of the parameters of the beacon symbol (diffusion coefficient, emission and threshold levels) can satisfactorily mitigate the effects of framing errors and provide a close performance to the molecular channel with perfect synchronization. Therefore, we conclude that there may be no need for synchronizing the transmitter and receiver clocks if a beacon symbol is introduced and properly designed.

In order to complete the development of MASC, our future work is to investigate the effects of clock skew, which is the relative drift between the transmitter and receiver local clocks. We expect that the joint effects of random propagation and clock skew will demand for structuring the transmitter-receiver communication in the form of short beacon-headed messages at a predefined frequency. Another future work would consist of extending our analysis to more realistic channel conditions, which would entail the use of mechanisms to obtain reliable channel estimates, as well as the adjustment of the emission levels of symbols in response to

these estimates. These mechanisms should also account for the ISI effects caused by arbitrary levels of channel memory.

REFERENCES

- [1] R. A. Freitas, "Nanomedicine, basic capabilities," in *Landes Bioscience*, vol. 1. Georgetown, TX, USA: 1999.
- [2] S. Hiyama, Y. Moritani, T. Suda, R. Egashira, A. Enomoto, M. Moore, and T. Nakano, "Molecular communication," in *Proc. NSTI Nanotech*, Anaheim, CA, USA, 2005, p. 162.
- [3] I. F. Akyildiz, F. Brunetti, and C. Blazquez, "Nanonetworking: A new communication paradigm," *Comput. Netw.*, vol. 52, no. 12, pp. 2260–2279, Jun. 2008.
- [4] T. Nakano, A. W. Eckford, and T. Haraguchi, *Molecular Communication*. Cambridge, U.K.: Cambridge Univ. Press, 2013.
- [5] B. Atakan, *Molecular Communications and Nanonetworks: From Nature To Practical Systems*. New York, NY, USA: Springer-Verlag, 2014.
- [6] T. Nakano, M. J. Moore, F. Wei, A. V. Vasilakos, and J. Shuai, "Molecular communication and networking: Opportunities and challenges," *IEEE Trans. Nanobiosci.*, vol. 11, no. 2, pp. 135–148, Jun. 2012.
- [7] I. Llatser, A. Cabellos-Aparicio, and E. Alarcon, "Networking challenges and principles in diffusion-based molecular communication," *IEEE Wireless Commun.*, vol. 19, no. 5, pp. 36–41, Oct. 2012.
- [8] M. Kuran, T. Tugcu, and B. Edis, "Calcium signaling: Overview and research directions of a molecular communication paradigm," *IEEE Wireless Commun.*, vol. 19, no. 5, pp. 20–27, Oct. 2012.
- [9] B. Atakan, O. Akan, and S. Balasubramaniam, "Body area nanonetworks with molecular communications in nanomedicine," *IEEE Commun. Mag.*, vol. 50, no. 1, pp. 28–34, Jan. 2012.
- [10] S. Abadal and I. F. Akyildiz, "Bio-inspired synchronization for nanocommunication networks," in *Proc. IEEE Global Telecommun. Conf.*, Dec. 2011, pp. 1–5.
- [11] M. J. Moore and T. Nakano, "Oscillation and synchronization of molecular machines by the diffusion of inhibitory molecules," *IEEE Trans. Nanotechnol.*, vol. 12, no. 4, pp. 601–608, Jul. 2013.
- [12] L. Lin, F. Li, M. Ma, and H. Yan, "Synchronization of bio-nanomachines based on molecular diffusion," *IEEE Sensors J.*, vol. 16, no. 19, pp. 7267–7277, Oct. 2016.
- [13] L. Lin, C. Yang, M. Ma, and S. Ma, "Diffusion-based clock synchronization for molecular communication under inverse Gaussian distribution," *IEEE Sensors J.*, vol. 15, no. 9, pp. 4866–4874, Sep. 2015.
- [14] L. Lin, C. Yang, M. Ma, S. Ma, and H. Yan, "A clock synchronization method for molecular nanomachines in bionanosensor networks," *IEEE Sensors J.*, vol. 16, no. 19, pp. 7194–7203, Oct. 2016.
- [15] Z. Luo, L. Lin, and M. Ma, "Offset estimation for clock synchronization in mobile molecular communication system," in *Proc. IEEE Wireless Commun. Netw. Conf.*, Apr. 2016, pp. 1–6.
- [16] L. Lin, J. Zhang, M. Ma, and H. Yan, "Time synchronization for molecular communication with drift," *IEEE Commun. Lett.*, vol. 21, no. 3, pp. 476–479, Mar. 2017.
- [17] H. Shahmohammadian, G. G. Messier, and S. Magierowski, "Blind synchronization in diffusion-based molecular communication channels," *IEEE Commun. Lett.*, vol. 17, no. 11, pp. 2156–2159, Nov. 2013.
- [18] V. Jamali, A. Ahmadzadeh, and R. Schober, "Symbol synchronization for diffusion-based molecular communications," *IEEE Trans. Nanobiosci.*, vol. 16, no. 8, pp. 873–887, Dec. 2017.
- [19] Z. Luo, L. Lin, W. Guo, S. Wang, F. Liu, and H. Yan, "One symbol blind synchronization in SIMO molecular communication systems," *IEEE Wireless Commun. Lett.*, vol. 7, no. 4, pp. 530–533, Aug. 2018.
- [20] C. Lo, Y.-J. Liang, and K.-C. Chen, "A phase locked loop for molecular communications and computations," *IEEE J. Sel. Areas Commun.*, vol. 32, no. 12, pp. 2381–2391, Dec. 2014.
- [21] Y.-K. Lin, W.-A. Lin, C.-H. Lee, and P.-C. Yeh, "Asynchronous threshold-based detection for quantity-type-modulated molecular communication systems," *IEEE Trans. Mol. Biol. Multi-Scale Commun.*, vol. 1, no. 1, pp. 37–49, Mar. 2015.
- [22] B. Atakan, S. Galmés, and O. B. Akan, "Nanoscale communication with molecular arrays in nanonetworks," *IEEE Trans. Nanobiosci.*, vol. 11, no. 2, pp. 149–160, Jun. 2012.
- [23] W. Haselmayr, N. Varshney, A. T. Asyari, A. Springer, and W. Guo, "On the impact of transposition errors in diffusion-based channels," *IEEE Trans. Commun.*, vol. 67, no. 1, pp. 364–374, Jan. 2019.

- [24] Y.-P. Hsieh, Y.-C. Lee, P.-J. Shih, P.-C. Yeh, and K.-C. Chen, "On the asynchronous information embedding for event-driven systems in molecular communications," *Nano Commun. Netw.*, vol. 4, no. 1, pp. 2–13, Mar. 2013.
- [25] Q. Li, "The clock-free asynchronous receiver design for molecular timing channels in diffusion-based molecular communications," *IEEE Trans. Nanobiosci.*, vol. 18, no. 4, pp. 585–596, Oct. 2019.
- [26] N. Farsad, Y. Murin, W. Guo, C.-B. Chae, A. W. Eckford, and A. Goldsmith, "Communication system design and analysis for asynchronous molecular timing channels," *IEEE Trans. Mol. Biol. Multi-Scale Commun.*, vol. 3, no. 4, pp. 239–253, Dec. 2017.
- [27] F. Dressler and S. Fischer, "Connecting in-body Nano communication with body area networks: Challenges and opportunities of the Internet of Nano Things," *Nano Commun. Netw.*, vol. 6, no. 2, pp. 29–38, Jun. 2015.
- [28] J. Laothawornkitkul, J. E. Taylor, N. D. Paul, and C. N. Hewitt, "Biogenic volatile organic compounds in the Earth system," *New Phytologist*, vol. 183, no. 1, pp. 27–51, Jul. 2009.
- [29] I. Karatzas and S. E. Shreve, *Brownian Motion and Stochastic Calculus*. New York, NY, USA: Springer, 1991.
- [30] S. Galmes and B. Atakan, "Performance analysis of diffusion-based molecular communications with memory," *IEEE Trans. Commun.*, vol. 64, no. 9, pp. 3786–3793, Sep. 2016.



BARIS ATAKAN received the B.Sc. degree from Ankara University, Ankara, Turkey, in 2000, the M.Sc. degree from Middle East Technical University, Ankara, in 2005, and the Ph.D. degree from the Next-Generation and Wireless Communications Laboratory, School of Sciences and Engineering, Koç University, Istanbul, Turkey, in 2011, all in electrical and electronics engineering. He is currently an Associate Professor with the Department of Electrical and Electronics Engineering, İzmir Institute of Technology, İzmir, Turkey. His current research interests include nanoscale and molecular communications, nanonetworks, and biologically inspired communications.



SEBASTIÀ GALMÉS received the M.Sc. degree in electrical engineering from the Polytechnic University of Catalonia, Barcelona, Spain, in 1989, and the Ph.D. degree in computer science from the University of Balearic Islands, Palma de Mallorca, Spain, in 1999. He is currently an Associate Professor with the Department of Mathematics and Computer Science, University of Balearic Islands. He has recently joined the Health Research Institute of the Balearic Islands (IdISBa). His current research interests focus on wireless communications, wireless sensor networks, nanoscale and molecular communications, and the application of nanonetworks to health care.

• • •